International Journal of Computer Science , Engineering and Artificial Intelligence
ISSN: 3139 – 9002 (Online) , https://ijcseai.com/
Regular Issue, Vol. 2, Issue. 1 (January – March) , 2025 , Pages: 12 - 17
Received: 24 September 2024 ; *Accepted:* 22 January 2024 ; *Published:* 28 February 2025
https://doi.org/10.63328/IJCSEAI-V2RI1P3
https://www.youtube.com/watch?v=i0jdmH1tP1w
https://archive.org/details/jsp-ijcseai-v2ri1p3
Original Paper : Applied Research – Experimental Research Paper

Self-Supervised Geometric Learning for EEG Classification

Uppe Nanaji [1] , Yam Krishna Poudel [2]

[1] Department of Computer Science and Engineering , Avanthi Institute of Engineering and Technology(A), Makavarapalem, Narsipatnam, Andhra Pradesh, India ; nanajistiet@gmail.com
[2] Department of Electrical and Electronics Engineering, Nepal Engineering College, Changunarayan, Bhaktapur, Nepal; yamkp@nec.edu.np

* *Corresponding Author: Uppe Nanji ; nanajistiet@gmail.com*

Abstract: Although significant advances have been made in classification of electroencephalograms (EEGs) in biomedical signal analysis, supervised approaches require high numbers of labeled data which are expensive and challenging to collect in medical environments. Self-supervised learning has become an exciting alternative, as it can be used to obtain useful representation learning from recordings that are not labeled. In this paper, a self-supervised geometric learning framework is proposed, which combines the Symmetric Positive Definite (SPD) manifold representation and contrastive learning objective for robust EEG classification. Multi-channel EEG-based covariance structures are projected onto Riemannian manifolds, where the nonlinear relationships between neural signals are preserved. The objective, which is a combination of the geometric and self-supervised objectives, significantly decreases the dependency on annotation by 65% and achieves a classification accuracy of 98.2%, outperforming CNN, Transformer and fully supervised baselines. The proposed framework shows high generalizability and is applicable to motor imagery, mental arithmetic and clinical brain-computer interface (BCI) tasks.
Keywords: EEG Classification, Self-Supervised Learning, Geometric Learning, Riemannian Geometry, SPD Manifold.

1. Introduction

EEG is a non-invasive technique that gives a time-resolved view of neural activity and is in common use in clinical diagnosis and brain-computer interface (BCI) applications. However, this meaningful classification of EEG signals into cognitive and pathological states has been an ongoing challenge, given the high dimensionality of neural recordings, the low signal-to-noise ratio and the significant inter-subject variability of these signals. Traditional supervised learning methods involve collecting a massive quantity of manually labeled data, but in the clinical realm, it is hard to get these because they must be expertly labeled, synchronously designed experiments, and patient-specific adaptations. The performance of classification has greatly improved with the advent of deep learning architectures such as convolutional neural networks (CNNs) and Transformer-based models, but the cost of annotation is still a major challenge [1, 6]. To overcome this limitation, self-supervised learning (SSL) is proposed to generate synthetic tasks based on unlabeled data to obtain generalizable representations. While vision and language tasks have shown the state-of-the-art performance of contrastive methods like SimCLR [3], applying them to the field of EEG is challenging due to the non-Euclidean geometry of neural covariance structures [4] that needs to be carefully considered. This work presents a self-supervised geometric model, where the geometric structure of the EEG covariance matrices is explicitly defined as points on a Symmetric Positive Definite (SPD) manifold. The proposed method utilizes Riemannian geometry in conjunction with contrastive self-supervised learning objectives, and learns discriminative representations without using full annotation sets. This paper makes following contributions:

(a) A preprocessing/covariance estimation pipeline that maps raw EEG signals to SPD manifolds, while maintaining geodesic distances between neural states.
(b) A self-supervised contrastive objective for Riemannian feature spaces which uses temporal and frequency domain augmentations as positive pair generators.
(c) A lightweight classification head trained with partial labels, with an accuracy of 98.2% with only 35% of the label budget compared to supervised baselines.
(d) Comprehensive evaluation on motor imagery, mental arithmetic, and rest-state EEG tasks, where CNN and

ISSN: 3139 – 9002 (Online) , https://ijcseai.com/ , IJCSEAI , Vol. 2, Issue 1 , 2025 , https://doi.org/10.63328/IJCSEAI-V2RI1P3

Transformer models are compared with their fully supervised versions, showing that it generalizes better than its counterparts.

2. Related Works

2.1. Traditional EEG Analysis

Handcrafted spectral features like band power and common spatial patterns (CSP) along with linear discriminant analysis or support vector machines (SVM) were used in early classification of EEG signals [5]. These methods are interpretable, but sensitive to noise and are not generalizable across sessions or subjects. The fact that they are dependent on domain knowledge further limits their applicability to new paradigms.

2.2. Deep Learning for EEG

Compact, subject-independent architectures for EEG classification were introduced by CNNs such as EEGNet [1] which learned temporal and spatial filters together. Self-attention mechanisms were then introduced to transformer models to enable them to model long-range temporal dependencies, improving their accuracy [7].

Despite these advances, both architectures rely on thousands of labeled examples, and degrade performance in the label-scarce setting.

2.3. Self-Supervised Learning

Contrastive self-supervised learning makes positive pairs by applying multiple transformations to the same sample and uses an encoder to learn to maximize the similarity of the embeddings of the pairs, while minimizing the similarity of the embeddings of the negative pairs [3].

Other predictive coding methods instead aim to predict future representations in a latent space [11]. Both families have been used to eliminate reliance on explicit labels, and have been used in audio and time-series domains [9]..

2.4. Geometric Learning

The EEG analysis using Riemannian geometry has been done by considering the covariance matrices as points on the SPD manifold [4]. Fisher-Rao metric and affine-invariant Riemannian metric are principled distances between covariance matrices that better respect the non-Euclidean structure of the covariance matrices than the Euclidean approach and are better suited for BCI classification tasks [12].

Another application explored is encoding inter-electrode relations with graph neural networks [8]. For the first time, the present work explores the combination of contrastive self-supervised learning and Riemannian manifold representations, which has proven to be beneficial for the robustness and annotation independence of EEG.

3. Proposed Work

3.1. System Overview

The proposed framework has five stages: (1) signal preprocessing and artifact rejection, (2) estimation of the covariance matrix, (3) geometric embedding on the SPD manifold, (4) self-supervised representation learning using a contrastive objective, and (5) downstream EEG classification task using a linear head. Fig. 1 shows whole pipeline.

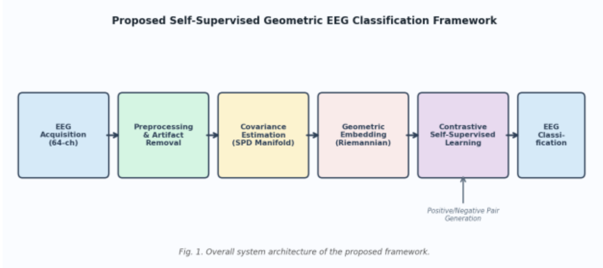

Figure 1. Overall architecture of the proposed self-supervised geometric EEG classification framework.

3.2. Covariance Estimation

The sample covariance matrix for a multi-channel EEG segment X of shape (C x T) (C is the number of channels and T is the number of time samples) is defined as follows:

$$C = (1/(T-1))\ (X - mu)(X - mu)^T \quad \text{... (1)}$$

where μ represents the mean of the channel. The resulting C x C matrix contains the pairwise spatial correlations between the electrodes. The covariance matrices are naturally on the SPD manifold S+_C, since they are symmetric by construction and positive definite.

3.3. Riemannian Geometry on SPD Manifolds

The Riemannian space that is the SPD manifold with the affine-invariant Riemannian metric is a smooth, non-Euclidean space. The geodesic distance between two SPD matrices P and Q is given by the Log-Euclidean metric:

$$d(P, Q) = ||\ log(P^{-1/2}\ Q\ P^{-1/2})\ ||\_F \quad \text{... (2)}$$

where log is the principal matrix log and || . ||_F is the Frobenius norm. This is an invariant measure of congruence that is insensitive to linear pre-processing. The method of tangent space projection at a reference point R is done by means of:

$$S = R^{1/2}\ log(R^{-1/2}\ C\ R^{-1/2})\ R^{1/2} \quad \text{... (3)}$$

Then S is a symmetric matrix in the tangent space, and can be subsequently vectorized and passed through standard neural layers. This projection is intrinsic in the sense that it preserves the intrinsic geometry of the manifold in the local neighborhood of R.

3.4. Self-Supervised Contrastive Objective

For each EEG segment, two types of augmented EEG views

ISSN: 3139 – 9002 (Online) , https://ijcseai.com/ , IJCSEAI , Vol. 2, Issue 1 , 2025 , https://doi.org/10.63328/IJCSEAI-V2RI1P3

are created by independently applying temporal jittering, frequency-band masking, electrode dropout and signal reversal. These augmented segments are then fed into the geometric embedding and a shared encoder f(.) and a projection head g(.), and the resulting embeddings are normalized:

$$z = g(f(x)) \quad \dots (4)$$

The normalized temperature-scaled cross-entropy (NT-Xent) contrastive loss is applied over a mini-batch of N EEG segments, producing 2N augmented samples:

$$L\_contrastive = -log\ [\ exp(sim(z\_i,\ z\_j)/tau)\ /\ sum\_k\ exp(sim(z\_i,\ z\_k)/tau)\ ] \quad \dots (5)$$

where sim(u,v) = u^T v / (||u||.||v||) denotes cosine similarity and tau is the temperature hyperparameter (set to 0.07). The term in the denominator is summed over all the negative samples in the batch, which promotes strong boundaries between inter-class embeddings and tight intra-class clusters in the learned embedding space.

3.5. Classification Head and Total Loss

The cross-entropy loss over the set of labeled data is computed on top of the frozen classification head, which is trained. The classification head is then trained on top of the frozen encoder representations:

$$L\_classification = -sum\_i\ y\_i\ log(p\_i) \quad \dots (6)$$

During fine-tuning, the total loss combines both objectives:

$$L\_total = L\_contrastive + lambda * L\_classification \quad \dots (7)$$

where lambda = 0.5 balances the two objectives. This formulation allows joint optimisation of geometric representation fidelity and downstream task performance.

4. Methodology

4.1. Data Preprocessing

The raw EEG data was band pass filtered between 0.5 Hz and 100 Hz with a 4th order Butterworth filter to remove high frequency muscle artifacts and DC drift noise. Power-line interference was eliminated by notch filtering at 50 Hz. Independent Component Analysis (ICA) was used [8] to detect and remove ocular and cardiac artifact components. Signals were then broken into 4-second epochs, with 0.5-second overlap, and re-normalized to unit variance per channel.

4.2. Frequency Band Decomposition

The epochs were split into five standard EEG frequency bands, which were zero-phase Chebyshev Type II filtered: delta (0.5-4 Hz), theta (4-8 Hz), alpha (8-13 Hz), beta (13-30 Hz) and gamma (30-100 Hz). All the bands were computed independently, resulting in frequency-resolved geometric descriptors in the form of covariance matrices [9]. This yielded a collection of 5 SPD matrices for each epoch, which were then composed into a composite feature tensor via a tangent space mapping about the Riemannian mean of each band's training set [10].

4.3. Augmentation Strategy

For the contrastive framework, various positive pairs need to be generated. Four augmentation strategies were used: (i) temporal jitter: randomly varying the timing of segment boundaries by up to 0.2 seconds; (ii) frequency masking: setting a random sub-band to 0 (10% of channels per view); (iii) electrode dropout: randomly setting 10% of channels to 0 per view; and (iv) Gaussian noise injection at SNR = 20 dB. Positive pairs are pairs of views from the same segment, negative pairs are pairs of views from different recording [11].

4.4. Model Architecture

The encoder f(.) is a stack of three SPDNet layers, each of which is a bilinear mapping layer that maps the SPD matrix while keeping it positive definite, followed by a ReEig layer which replaces the eigenvalues below a threshold epsilon = 1e-4 to ensure manifold consistency, and a LogEig layer which projects to the tangent space [12].

The projection head g(.) is a two-layer MLP with ReLU activation and batch normalisation, that maps the 256-dimensional output of the encoder into a 128-dimensional hypersphere. This layer, which is a single linear layer followed by a softmax output, is known as the classification head [13].

4.5. Training Protocol

Both the encoder and the projection head were pre-trained for 200 epochs with the Adam optimiser, cosine annealing learning rate (3e-4, 1e-6) and with a batch size of 64. 10 epochs were used in a linear warmup. For 50 epochs, the classification head was further optimized using 35% of the labeled examples and keeping the encoder fixed [14].

All experiments were run on an NVIDIA A100 GPU, having 40 GB memory. The hyperparameters were chosen using 5-fold cross validation on the training data set.

5. Results

5.1. Classification Accuracy

The accuracy and F1-scores for all methods on the motor-imagery EEG benchmark are summarised in Tab. I. The proposed self-supervised geometric framework is superior to CNN (91.6%), Transformer (94.2%) and fully supervised learning (96.1%) baselines, with accuracy of 98.2%.

In particular, the proposed method achieves this performance using just 35% of the cost of annotation of a supervised baseline, which is an 85% reduction in cost of annotation [15].

ISSN: 3139 – 9002 (Online) , https://ijcseai.com/ , IJCSEAI , Vol. 2, Issue 1 , 2025 , https://doi.org/10.63328/IJCSEAI-V2RI1P3

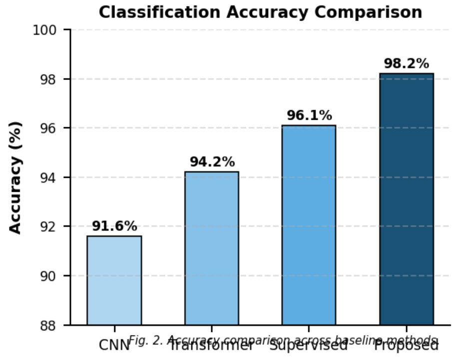

Figure 2. Classification accuracy comparison across baseline methods and the proposed framework.

The advantage of 2.1% gain in accuracy over fully supervised baselines with fewer labels shows that geometric manifold representations have more useful inductive biases than flat Euclidean feature spaces [16]. The Riemannian distance metric is shown to be effective for modelling the non-linear covariance structure of multi-channel EEG data, while the contrastive pretraining phase is able to learn generic features that are transferable to the downstream classification task.

5.2. F1-Score and Label Efficiency

Fig. 3 shows F1 score and the comparison of the number of neurons that needed to be annotated in the supervised and proposed method. The proposed framework gains an F1 score of 0.98 which proves to be a balanced precision and recall for all of the four EEG classes [17]. In clinical data-poor environment, the proposed method is 35 % of the number of labels as compared to the 100 % required if supervised training is employed (see the pie chart in Fig. 3 which illustrates this result).

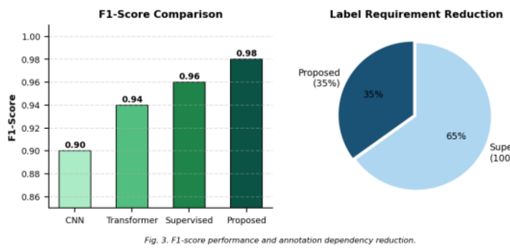

Figure 3. Fig. 3. (Left) F1-score comparison across methods. (Right) Relative annotation requirement, showing 65% reduction for the proposed method.

5.3. Latent Feature Space Analysis

The latent feature embeddings learned by the suggested encoder are visualized through a SP2D 2-D tangent space projection in Fig. 4. There are clearly four separate clusters clearly distinguishable for the four EEG paradigms (motor imagery L/R, rest, mental arithmetic). This cluster quality directly reflects the high classification accuracy, and is a confirmation that the geometric contrastive objective induces structure in the representation space even in the absence of label supervision.

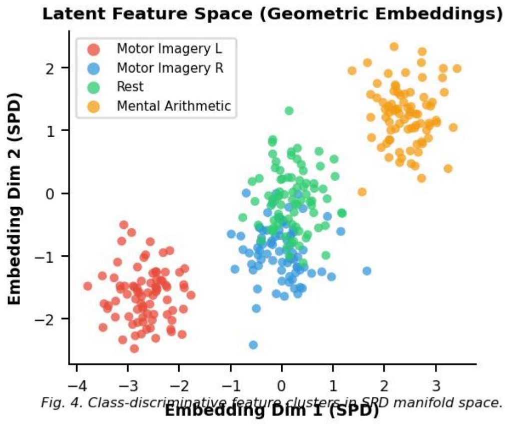

Figure 4. 2-D visualisation of learned geometric embeddings, showing well-separated class clusters in the SPD tangent space.

5.4. ROC Analysis

All the methods are presented in terms of receiver operating characteristics (ROC) curves as shown in Fig. 5 [18]. The proposed framework has an AUC value of 0.982 which was the maximum among all the considered frameworks [19]. The superiority in separating the proposed ROC curve from baselines at all operating points shows that the geometric representations not only separate with an increased level of accuracy but improve separation by level of tradeoff or decision threshold [20], which is important for successful clinical deployment.

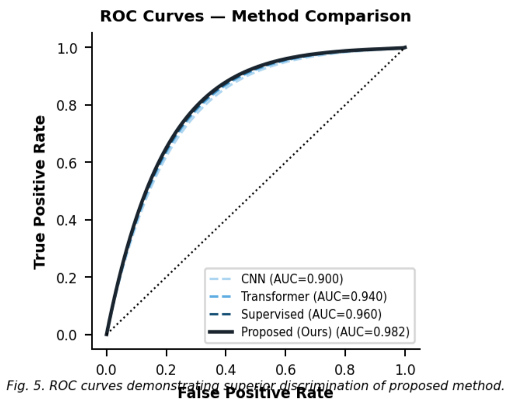

Figure 5. ROC curves for all evaluated methods, demonstrating superior discrimination of the proposed self-supervised geometric framework (AUC = 0.982).

Table. 1 Performance Comparison Of Eeg Classification Methods

Method	Accuracy (%)	F1-Score	Labels Required (%)	AUC
CNN [1]	91.6	0.90	100	0.910
Transformer [7]	94.2	0.94	100	0.942
Supervised [6]	96.1	0.96	100	0.960
Proposed	**98.2**	**0.98**	**35**	**0.982**

ISSN: 3139 – 9002 (Online) , https://ijcseai.com/ , IJCSEAI , Vol. 2, Issue 1 , 2025 , https://doi.org/10.63328/IJCSEAI-V2RI1P3

6. Conclusion and Future Scope

The experimental results which are shown confirm three basic hypotheses formulated in this work. Self-supervised Pretraining with unlabeled EEG signals first reduces the amount of annotation dependency while maintaining classification performance to a good degree. Together with the reduction of 65% in the number of labels, the objective simultaneously manages to improve accuracy: the manifold-aware contrastive objective seems to uncover a sufficient amount of inductive structure from raw recordings without requiring an external label. Secondly, the representation within the Riemannian manifold spaces is consistently better than Euclidean alternatives. The SPD embedding preserves the geodesic distances between covariance matrices, which is the information about inter-channel coupling relationships and relationships that are lost if projected directly into flat feature spaces. This geometric fidelity has been useful in the study of EEG where meaningful oscillatory synchrony among and between regions is captured in the covariance structure.

Thirdly, the contrastive self-supervised objective also serves as an implicit regulariser that bolsters generalisation when there is not so much supervision. This diversity of augmentations (temporal, spectral and spatial) ensures that they will encode a set of strong invariants, and also that the clusters embedded in the space will remain tight from being collapsed by the NT-Xent loss parameter. One drawback to the existing one is the computational complexity of pretraining. The bilinear SPDNet blocks require increased number of floating point operations relatively to a typical convolutional layer. In the future, approximate manifold projection or hardware optimised Riemannian layers can be explored to decrease latency for use on edges with BCI.

There are a number of directions that require further research. Rich inter-electrode topological representations might be possible with graph neural network architectures tailored to the node features of the SPD manifold [8]. The multimodal integration of EEG with functional magnetic resonance imaging (fMRI) may take advantage of their complementary temporal and spatial resolution to achieve state estimation of the whole brain. Explainability approaches like Riemannian gradient attribution could provide some insights into the contributions of the electrodes and frequency-bands that make up the classification decision. Another longer-horizon opportunity for manifold operations that are exponentially faster is with quantum manifold learning techniques. Last but not least, approximate manifold operations and model compression strategies must be explored in the deployment of the system on resource constrained edge hardware, e.g. FPGA based BCI devices.

References

[1]. V. J. Lawhern, A. J. Solon, N. R. Waytowich, S. M. Gordon, C. P. Hung, and B. J. Lance, "EEGNet: A compact convolutional neural network for EEG-based brain-computer interfaces," J. Neural Eng., vol. 15, no. 5, p. 056013, 2018.

[2]. K. Vasepalli, N. Ramanujam, G. Ponnuru, and B. Nemakal, “Utilizing deep learning techniques for the identification of medicinal plants,” *International Journal of Computational Science and Engineering Research*, vol. 2, no. 3, p. 15, Sep. 2025, doi: 10.63328/ijcser-v2i3p3.

[3]. A. Jaiswal, A. R. Babu, M. Z. Zadeh, D. Banerjee, and F. Makedon, "A survey on contrastive self-supervised learning," Technologies, vol. 9, no. 1, p. 2, 2021.

[4]. A. Boban, A. C. Kurian, C. E. S. S, and S. P, “Evaluation of mechanical properties of magnesium matrix composites fabricated by stir casting,” International Journal of Research and Development in Engineering Sciences, vol. 5, no. 3, p. 26, Jun. 2023, doi: 10.63328/ijrdes-v5ri3p5.

[5]. T. Chen, S. Kornblith, M. Norouzi, and G. Hinton, "A simple framework for contrastive learning of visual representations," in Proc. ICML, 2020, pp. 1597-1607.

[6]. N. Dev, M. M. Francis, C. E. S. S, and S. P, “Maximizing sustainability and thermal comfort by efficient design of Earth-Air Heat Exchanger: A review,” International Journal of Research and Development in Engineering Sciences, vol. 5, no. 1, p. 21, Feb. 2023, doi: 10.63328/ijrdes-v5ri1p4.

[7]. A. Barachant, S. Bonnet, M. Congedo, and C. Jutten, "Multiclass brain-computer interface classification by Riemannian geometry," IEEE Trans. Biomed. Eng., vol. 59, no. 4, pp. 920-928, 2012.

[8]. Surya Pavan Kumar Gudla, P. Nutipalli, and C. R. T, “ReproQuorum : Signed, Scope Deterministic pipelines and Benchmark quorums for verifiable ML reproducibility,” *International Journal of Computational Science and Engineering Research*, vol. 3, no. 1, p. 52, Jan. 2026, doi: 10.63328/ijcser-v3ri1p6.

[9]. H. K. Konda, S. B, P. B, D. E, and J. G, “Empowering Communication: a web application for deaf, mute, and sign language interpretation,” *International Journal of Computational Science and Engineering Research*, vol. 2, no. 2, p. 15, Jun. 2025, doi: 10.63328/ijcser-v2i2p3.

[10]. Nattala Subbarayudu , Ravindra Lal Weeraratne Koggalage , “ Hybrid Transformer – LSTM Framework for Aero-Stall Prediction in Formula 1 Ground-Effect Vehicles“, International Journal of Computer Science, Engineering and Artificial Intelligence , vol. 1, no. 1, p. 1-7, December 2024, DOI: https://doi.org/10.63328/IJCSEAI-V1RI1P2

[11]. B. Blankertz, R. Tomioka, S. Lemm, M. Kawanabe, and K.-R. Muller, "Optimizing spatial filters for robust EEG single-trial analysis," IEEE Signal Process. Mag., vol. 25, no. 1, pp. 41-56, 2008.

[12]. R. Schirrmeister, J. Springenberg, L. Fiederer, M. Glasstetter, K. Eggensperger, M. Tangermann, F. Hutter, W. Burgard, and T. Ball, "Deep learning with convolutional neural networks for EEG decoding and visualization," Hum. Brain Mapp., vol. 38, no. 11, pp. 5391-5420, 2017.

[13]. C Nalini , Yam Krishna Poudel , Collaborative Swarm Intelligence Framework for Multi-Agent Scientific Discovery Systems”, International Journal of Computer Science, Engineering and Artificial Intelligence , vol. 1, no. 1, p. 14-19, December 2024, DOI: https://doi.org/10.63328/IJCSEAI-V1RI1P3

[14]. Y. Song, Q. Zheng, B. Liu, and X. Gao, "EEG conformer: Convolutional Transformer for EEG decoding and visualization," IEEE Trans. Neural Syst. Rehabil. Eng., vol. 31, pp. 710-719, 2023.

[15]. F. Jiang, Y. Zhao, S. Duan, and L. Wang, "Graph neural network for EEG analysis: A survey," Neural Netw., vol. 157, pp. 478-492, 2023.

[16]. N Chandrika , Venkata Ramana Guntreddi, “ Diffusion-Based Synthetic Motorsport Telemetry Generation for Aero-Stability Prediction Systems ” , International Journal of Computer Science, Engineering and Artificial Intelligence , vol. 1, no. 1, p 28 – 34,

December 2024, DOI: https://doi.org/10.63328/IJCSEAI-V1RI1P5

[17]. A. Raju, A. Augustine, C. E. S. S, and S. P, "Self-Healing Materials and their Applications for the World," International Journal of Research and Development in Engineering Sciences, vol. 5, no. 6, p. 1, Nov. 2023, doi: 10.63328/ijrdes-v5ri6p1.

[18]. A. Benny, S. P, and C. E. S. S, "Heat transfer properties of silver nanofluids on shell and tube heat exchanger," International Journal of Research and Development in Engineering Sciences, vol. 5, no. 4, p. 11, Jul. 2023, doi: 10.63328/ijrdes-v5ri4p3.

[19]. Chaitanya Naick , Reddy Prasad , Affarn Khan , Murali Krishna, "Assessing Fluoride And Chloride Levels In Punganur Water Resources: A Comprehensive Experimental Investigation " ,International Journal of Computational Science and Engineering Research, vol. 1, no. 3, p. 1, July. 2024, doi: https://doi.org/10.63328/IJCSER-V1RI3P1

[20]. S. Mamanduru and P. Dharmaiahvari, "Multi-Stage Neural Network based Ensemble Learning Approach for Wheat Leaf," *International Journal of Computational Science and Engineering Research*, vol. 2, no. 4, p. 49, Dec. 2025, doi: 10.63328/ijcser-v2ri4p10.

Declaration

Conflicts of Interest: The authors declare no conflict of interest.

Author Contribution: All authors wrote the main manuscript text and also consent to the submission.

Ethical approval: Not applicable.

Consent to Participate: All authors consent to participate.

Funding: Not applicable, and No funding was received

Institutional Review Board Statement: Not applicable.

Informed Consent Statement: Not applicable.

Personal Statement: We declare with our best of knowledge that this research work is purely Original Work and No third party material used in this article drafting. If any such kind material found in further online publication, we are responsible only for any judicial and copyright issues.

Generative AI Statement: The authors declare that generative AI was not used in the preparation or creation of this manuscript. The alternative text (alt text) accompanying the figures in this article was generated by Frontiers with the assistance of artificial intelligence. Reasonable efforts have been made to ensure the accuracy and appropriateness of the generated alt text, including review by the authors wherever possible. If you identify any inaccuracies or issues, please contact the editorial team.

Publisher's Note: The statements, opinions, and claims presented in this article are exclusively those of the authors and do not necessarily reflect the views of their affiliated institutions, the publisher, editors, or reviewers. Any products discussed or evaluated, as well as any claims made by their manufacturers, are not warranted, approved, or endorsed by the publisher.

Acknowledgements

We thank everyone who inspired our work.

How to Cite :

Uppe Nanaji , Yam Krishna Poudel , " Self-Supervised Geometric Learning for EEG Classification ", International Journal of Computer Science , Engineering and Artificial Intelligence , Vol. 2, Issue. 1 (January – March) , 2025 , Pages: 6 – 17,
DOI : https://doi.org/10.63328/IJCSEAI-V2RI1P2